

Quarterly Report for  
**September 1998 - December 1998**  
**Stanford Geothermal Program**  
DE-FG07-95ID13370

## Table of Contents

<b>1. MEASUREMENTS OF STEAM-WATER RELATIVE PERMEABILITY</b>	<b>1</b>
1.1 INTRODUCTION	1
1.2 EXPERIMENTAL DESIGN	1
1.3 FUTURE WORK	3
<b>2. AN EXPERIMENTAL INVESTIGATION OF BOILING HEAT CONVECTION IN FRACTURES</b>	<b>4</b>
2.1 INTRODUCTION	4
2.2 EXPERIMENTAL PREPARATIONS	4
2.3 EXPERIMENTAL PROCEDURE	7
2.4 OBSERVATIONS	8
2.5 DISCUSSION	11
2.6 CONCLUSIONS	12
2.7 FUTURE RESEARCH	13
<b>3. EXPERIMENTAL DETERMINATION OF ENDPOINT SATURATION</b>	<b>14</b>
3.1 BACKGROUND	14
3.2 FUTURE PLANS	15
<b>4. REFERENCES</b>	<b>17</b>

# **1. MEASUREMENTS OF STEAM-WATER RELATIVE PERMEABILITY**

This research project is currently being conducted by Research Assistant Glenn Mahiya and Professor Roland Horne. The aim is to measure relative permeability relations for steam and water flowing simultaneously in rocks.

## **1.1 INTRODUCTION**

Steam-water relative permeability curves have been determined experimentally by Ambusso (1995) and Satik (1997) in the past under the Stanford Geothermal Program. An important concern, though, is that the repeatability of experimental results has not been established. Improvements in the experimental setup have been implemented, and we further these efforts with the installation of guard heaters to eliminate heat losses during the experiment. In the quarterly report for July–September 1998, we described in detail the flexible heaters that will be used for the experiment. These custom-made sheet heaters, each an array of independently controllable strip heaters, will compensate for whatever heat losses occur along the core and impose an adiabatic condition on the experiment. Eliminating the heat losses reduces the possible sources of errors, minimizes the time to reach equilibrium conditions, and allows for a larger two-phase zone over which saturations can be measured via the X-ray CT scanner.

In this report, we focus on the data acquisition and control system that we have developed to operate the flexible heaters.

## **1.2 EXPERIMENTAL DESIGN**

The general experimental setup has been discussed in the last quarterly report and can be visualized by referring to Figure 1.1. Note that the Kapton-insulated heaters are wrapped around the coreholder. In between the heaters and the coreholder, heat flux sensors are positioned along the core for measuring (net) heat loss. Each heat flux sensor is connected to a panel that interfaces with the National Instruments data acquisition hardware. Currently, we have three data acquisition modules installed. One SCXI-1100 module processes data from the pressure transducers, while an identical module reads temperature from thermocouple devices and heat fluxes from the sensors. The third module is the SCXI-1163R, a 32-channel, optically isolated, solid state relay that we are using to control the guard heaters. We use the software LabView to gather, process and display data, as well as control devices such as the heaters.

Figure 1.2 illustrates the setup that minimizes heat losses. Note that since heat loss varies with distance from the inlet of the core, the heat replenishment will likewise vary accordingly to attain zero net heat flux everywhere. Aside from spatial variation, heat loss also changes with time especially in the early part of the experiment when equilibrium has not been reached. Since the SCXI-1163R controls a device by switching it on or off, there is no direct way of providing variable power to the heater. It is not feasible to obtain a constant output from the heater that is different from the maximum it can deliver given since the voltage and current are fixed when the SCXI-1163R is used. Thus, a target level

of heat output is achieved by essentially switching the heater on and off (digital proportional control). The on-time and off-time are determined by the measurements made by the heat flux sensors. The LabView "virtual instrument", a graphical subroutine, that controls the flexible heaters is shown in Figure 1.3.

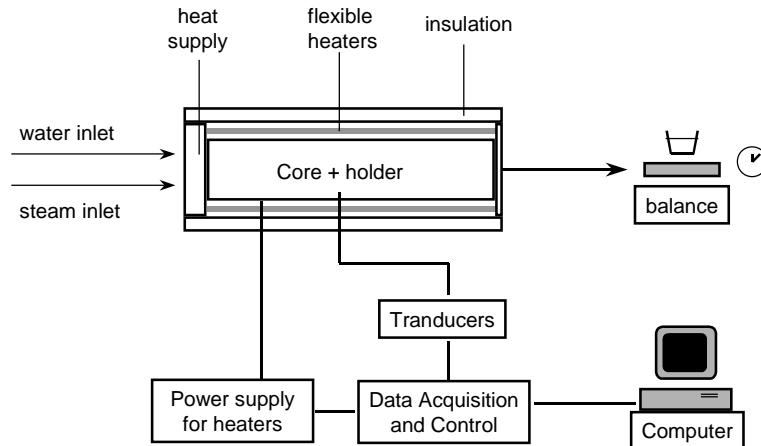


Figure 1.1: Schematic diagram of relative permeability experiment.

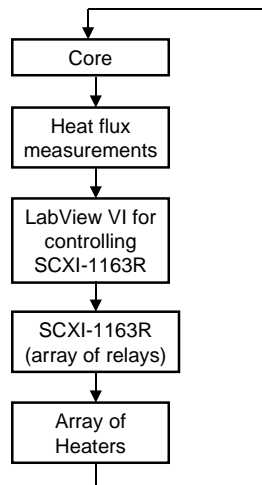


Figure 1.2: Control flow for flexible heaters.

A pulsing scheme shown in Figure 1.4 allows us to oscillate about the target heat flux with a small range of tolerable deviation set by the upper and lower limits. The heat flux measured serves as input to the sub-vi and is tested if it falls within the allowable range. If the value is within the range, the state of the heater (i.e., on or off) is not changed. Otherwise, an “on” signal will be sent if the heat flux falls below the lower limit, and an “off” signal is sent if the value goes beyond the upper limit. Since the heater has a finite characteristic response time (i.e., the time it requires to reach the maximum power) provides some advantage in that we do not always have to achieve the full power of the heater especially if the heat needed is well below the maximum deliverable output.

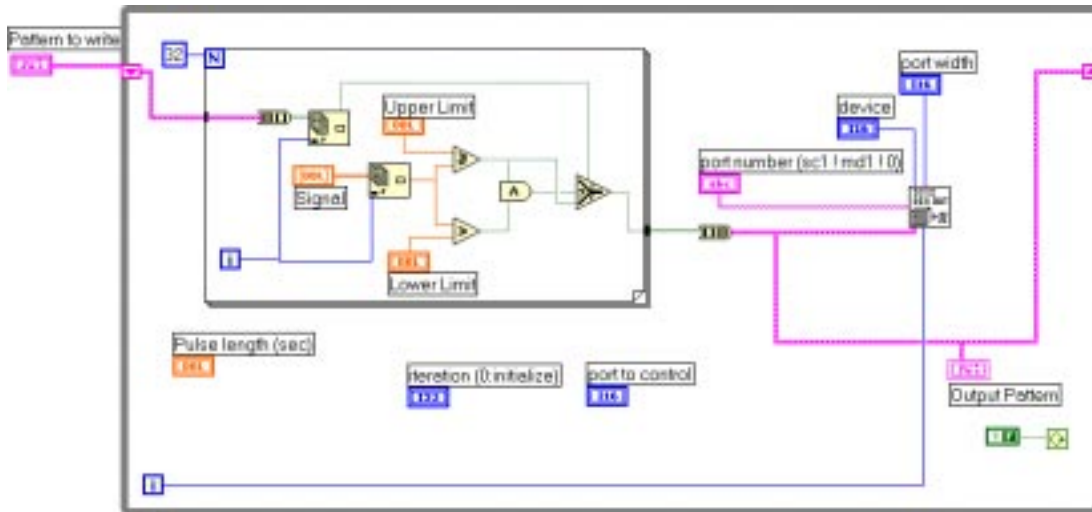


Figure 1.3: LabView virtual instrument for heater control.

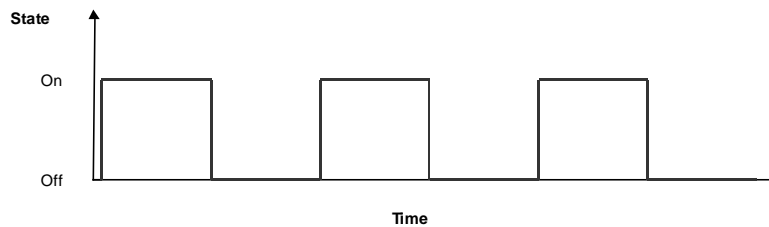


Figure 1.4: Pulsing scheme for controlling the guard heaters.

The advantage of using LabView is that results are displayed graphically in real time. This allows us to detect any abnormalities in the course of the experiment and correct them as necessary. From the continuous plot of heat flux sensor readings, it will be easy to see whether or not the flexible heaters are providing the appropriate amount of heat compensation.

### **1.3 FUTURE WORK**

Further improvements to the LabView subroutines for heater control are being made. We have yet to implement this modification to the experimental setup as we are still testing the reliability of control mechanism. We are currently preparing for an actual experiment in the X-ray CT scanner some time in the coming quarter. As part of this effort, heat flux sensors are being recalibrated to ensure accurate measurements. The original LabView routine used for the experiment is also being modified to incorporate the new subroutine for controlling the heat guards.

## **2. AN EXPERIMENTAL INVESTIGATION OF BOILING HEAT CONVECTION IN FRACTURES**

This project is being conducted by Research Assistants Robb Barnitt and Robert DuTeaux, and Prof. Roland Horne. The goal is to investigate and compare the heat flux and temperature gradients that develop during boiling with liquid injection into a fracture. Improved understanding and modeling of heat transfer in a fracture will ultimately lead to better strategies for injection into fractured geothermal reservoirs.

### **2.1 INTRODUCTION**

The experimental work conducted this quarter was a joint research effort building upon graduate work completed by Bob DuTeaux in September 1998. Work done previously by Bob Duteaux utilized samples of Geysers core (graywacke), whereas this recent work experimented with more porous (sandstone) and nonporous (aluminum) materials. The experimental apparatus used during the Geysers core experiments was used again with the sandstone and aluminum. The aim was to investigate and compare the heat flux and temperature gradients that develop during boiling with liquid injection into a radial fracture, and examine the differences in behavior dependant upon the nature of the fracture boundary matrix. These experiments were designed to quantify the heat flux associated with liquid water flashing to steam in a fracture, and to investigate the degree of coupling between the heat flux and the vapor fraction flowing in the fracture. The findings of this venture will be published and presented at the 24th Workshop on Geothermal Reservoir Engineering, Stanford University, Stanford, CA on January 26, 1999.

### **2.2 EXPERIMENTAL PREPARATIONS**

The apparatus illustrated in Figure 2.1 was designed to provide a uniform temperature on the bottom of the rock sample and to quantify the heat flux and temperature gradients associated with liquid water flashing to steam on the fracture surface.

#### **2.2.1 Prior Experiments Using Geysers Rock**

Figure 2.1 shows the apparatus used in earlier experiments using Geysers core rock. Thermocouples were placed between thin slices of rock resting on top of a heat flux sensor and the heating element box. On top of the rock a glass disk forms the upper boundary of a fracture whose aperture is controlled by placing small triangular shims along the outer edge of the disk. The glass disk on top has a hole at its center for the injection of fluid into the fracture.

Three thin Geysers rock disks were prepared with a surface grinder to achieve flat well-mated surfaces. Thermocouples were placed on the aluminum heater box, and at each interface between rock disks. The outer edge of the rock was sealed with epoxy and silicone to prohibit radial flow within the rock and to restrain radial heat conduction. The thermocouples were located on the interfaces between disks radially 1.5 centimeters from the center. The circular aluminum box and rock disks were 11.5 centimeters in diameter,

and the sides and bottom of the aluminum were insulated with fiber board insulation and coated on the outside with RTV silicone. Thus, both the heat flux and temperature gradient normal to the surface of the rock were measured near the center of the fracture.

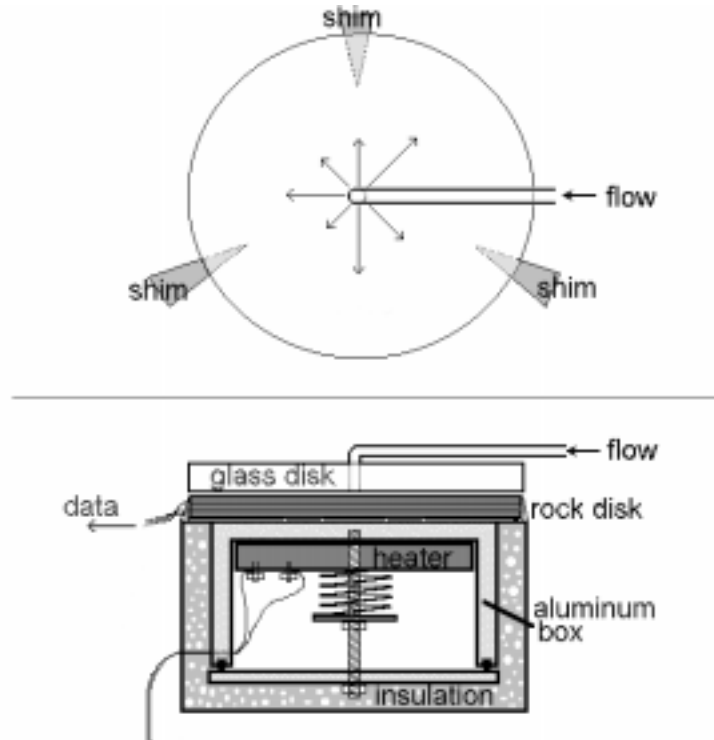


*Figure 2.1 Heat flux and temperature gradient measurement apparatus.*

To obtain a sufficient thermal contact with the rock, heat sink compound was used between the rock and the aluminum heater box. The rock surface closest to the heater was coated on the heater side with a thin film of high temperature epoxy to prevent the spontaneous imbibition of oil from the heat sink compound from entering the rock. The other surfaces were not treated except that shallow grooves were cut in the rock surfaces for the placement of thermocouples. The top surface of the heater box was engraved to hold the thermocouples and a heat flux sensor was placed on the base of the rock. On each of the surfaces where temperatures were recorded, three thermocouples were placed 1.5 cm radially out from the center, separated from one another by an angle of 120 degrees. Since the geometry is axisymmetric, two out of each set of thermocouples recorded redundant measurements. The rock disks were 3.10 mm, 4.19 mm, and 3.58 mm thick, from the bottom to the top respectively, and sets of three thermocouples were placed at each interface between the three disks.

### **2.2.2 Preparation of Sandstone and Aluminum Samples**

While the Geysers core was cut into thin slices with thermocouples placed between well mated surfaces, during the recent experiments, the aluminum disk and sandstone samples had small holes drilled at four different levels within the disk for a close tolerance fit of

the thermocouples. Again, the thermocouples were placed 1.5 cm radially out from the center. This is illustrated in Figure 2.2.

A better insulated copper heating element box was also prepared for the more recent experiments to constrain unwanted heat losses. The new heater box was machined to have two heat flux sensors on the surface above the electric heating element. This apparatus was designed to provide a uniform temperature and heat flux at the base of the rock.

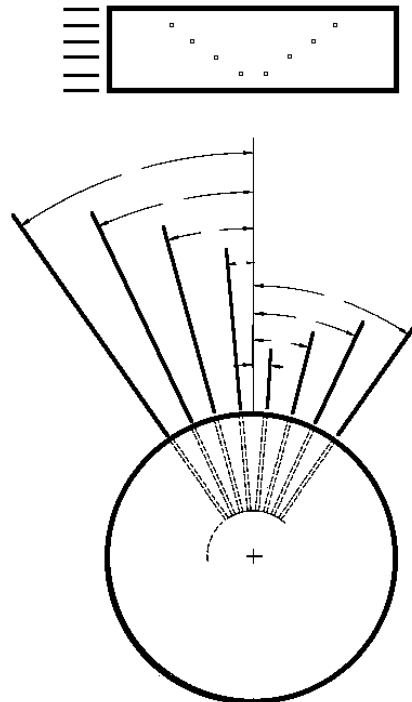


*Figure 2.2 Drilling and placement of thermocouples in sandstone and aluminum disks.*

As in the Geysers rock experiments, a glass disk was used in both assemblies to allow observation of the vapor fraction and flow characteristics, and a uniformly smooth circular fracture was created by compressing this glass disk against three small stainless steel shims.

The sandstone disk was machined circular and ground flat at 2 cm thick, and had epoxy applied to the bottom surface to prevent the oil from the thermally conductive paste from imbibing into the sample. Holes were drilled at levels 2.7 mm, 6.1 mm, 9.9 mm, and 13.5 mm from the top (fracture) surface. The aluminum disk was prepared similarly, except its total thickness was a little greater than 2.5 cm with holes drilled at four even increments about 5.1 mm from the bottom to the top surface. Stainless steel shims 0.508 mm thick were used to create an aperture of uniform dimension in these more recent experiments.



### **2.3 EXPERIMENTAL PROCEDURE**

The outer radial edge of the fracture was exposed to atmospheric pressure. The fracture was oriented horizontally and a small positive displacement pump was used to pump water through a copper coil immersed in boiling water to provide fluid at near saturated temperature. The pump was adjusted to supply discrete rates of 15, 30, and 60 ml/min, and the fracture aperture was fixed at 0.508 mm with both the sandstone and aluminum disks. The average flow velocity was thus varied by a factor of four. With liquid water these rates are well within the range of laminar flow. With boiling, however, the velocity was further increased as liquid flashed to vapor in the fracture.

Two types of experiments were conducted. The first was a single-phase experiment that was done to measure the thermal conductivity of the sample by comparing the heat flux measured with ice water injected into the fracture to the steady state temperature gradient. Assuming one-dimensional heat conduction, Fourier's law  $q'' = K \Delta T/L$  describes the relationship between the heat flux and the temperature gradient, where the proportionality factor  $K$  is the thermal conductivity of the rock. During the single-phase experiments temperatures were recorded at one minute intervals from each thermocouple location as ice water was pumped at 15, 30, and 60 ml/min.

The second type of experiment conducted was a steady-state boiling experiment with much higher temperatures and two-phase liquid and vapor flow in the fracture. During this experiment 70-100 volts and about 2.5 amps were supplied to the heater and maintained for the duration of the entire experiment. Again, temperatures were recorded every minute for many hours while the flow rate and fracture aperture were adjusted and the times of steady-state conditions were noted. Unfortunately the heat flux sensors failed during these experiments. At heat fluxes above  $10,000 \text{ W/m}^2$  the signal from the sensor either reached a maximum or dropped to zero and would not provide information on heat flowing across the sample disks. Therefore, the rock conductivity was calculated from the temperature gradient and the temperature change of the fluid in the previous single-phase experiments. This is possible because an energy balance between the rock and the fluid shows that the heat conducted through the rock increased the internal energy of the fluid, raising its temperature. Thus  $q'' = K \Delta T / \Delta X$  in the rock and  $q'' = (m C_p \Delta T) / A$  in the fluid, where  $K$  is the rock conductivity,  $\Delta T / \Delta X$  is the temperature gradient,  $m$  is the mass flow rate of the fluid,  $C_p$  is its heat capacity,  $\Delta T$  is the temperature gain of the fluid from inlet to outlet, and  $A$  is the surface area of the fracture.

This calculated rock conductivity was then used to calculate the heat fluxes from the temperature gradients in the boiling experiments. Again, we recognize that the temperature gradient varies with radial position and that the rock conductivity measured under lower temperature conditions is not accurate at higher temperatures with a mixture of liquid and vapor in the pores. Therefore, the absolute value of the heat fluxes is somewhat uncertain, but the relative magnitudes of heat fluxes under different flow conditions have been compared correctly.

## **2.4 OBSERVATIONS**

The single-phase steady state temperatures from earlier experiments with Geysers rock are plotted on Figure 2.3. While the average steady heat flux observed was  $11064 \text{ W/m}^2$ , a temperature drop of about  $130^\circ\text{C}$  was measured across the 10.9 mm net thickness of rock. The overall thermal conductivity of the three rock disks was calculated at  $0.92 \text{ W / m K}$ , while the bottom rock disk (which had the epoxy and thermally conductive paste applied to one surface) showed a value of  $0.53 \text{ W / m K}$ , and the middle and top rock disks both showed values of about  $1.24 \text{ W / m K}$ . While the bottom rock disk displays a thermal conductivity lower than the others, possibly due to its treatment with epoxy, the conductivity of the top two disks appears to be consistent, as indicated by the uniform slope of the temperature gradient in the plot.

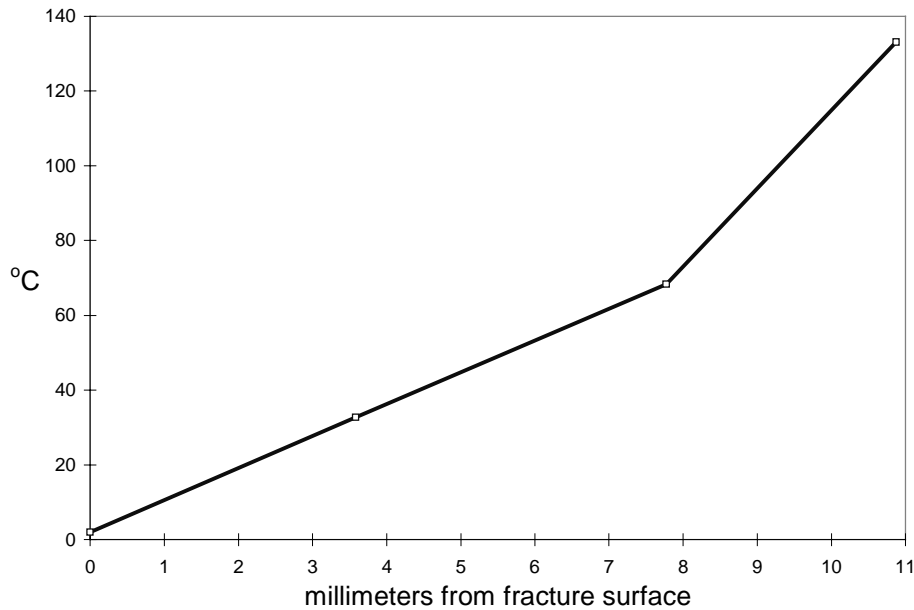


*Figure 2.3. Steady state temperature distribution with ice water injection.*

Data from the high temperature boiling flow experiment are shown in Figure 2.4. The arithmetic averages of temperatures from two steady states with water injected at 60 ml/min and 15 ml/min are displayed.

As noted earlier, the heat flux sensor read a continuous maximum after the apparatus was heated, so the heat flux was calculated indirectly from the temperature gradient and an assumed thermal conductivity. Assuming the internal thermal conductivity of  $1.25 \text{ W / m K}$  measured from the ice water experiment, a calculated heat flux of about  $25100 \text{ W/m}^2$  was observed to be practically independent of flow velocity and vapor fraction. Vapor fractions, however, never greatly exceeded about 40%.

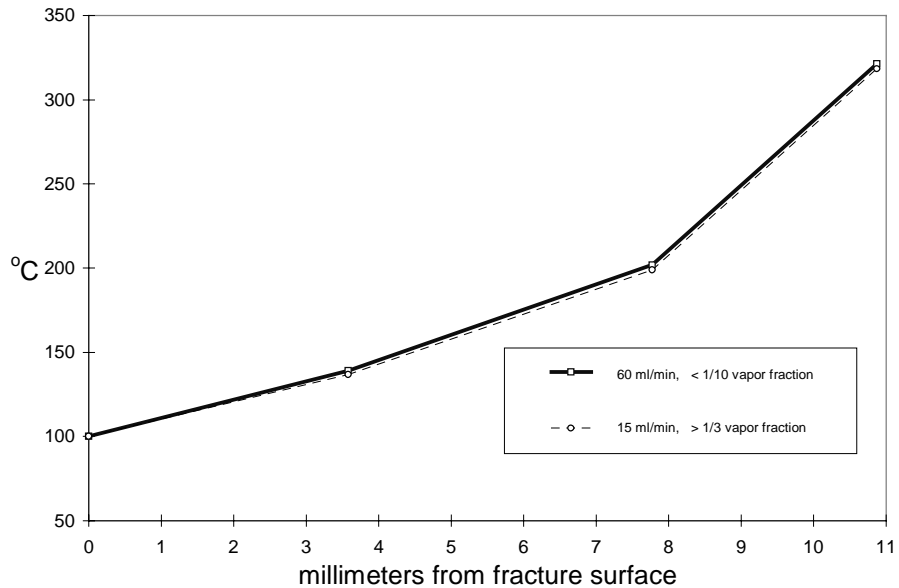


Figure 2.4. Steady state temperature distribution during injection / boiling flow.

Figure 2.5 plots the temperature gradients observed with boiling flow in the sandstone disk. Visual observation of this experiment revealed that the fracture aperture was not influencing the flow pattern to a great extent. The injected fluid penetrated into the sandstone at the center and exited predominantly along the outer edge. While observation and the internal temperatures indicated boiling, the temperature of the fluid measured at the perimeter of the fracture was a few degrees less than the saturated temperature. This indicates that not all of the fluid in the sandstone flowed at saturated temperature and that mixing at the outlet lowered the overall fluid outlet temperature.

During the experiment illustrated in Figure 2.5 another unusual result is illustrated in Table 5.1, which shows that the heat flux increased at the lower flow rates, presumably because more of the surface area of the fracture contained boiling flow. It appears that at higher flow rates not all pores in the fracture surface contained boiling flow, therefore the heat flux decreased.

Figure 2.6 plots the temperature gradient for the experiment with the aluminum disk. Although not easily seen on this scale, the slope of the temperature gradient increases slightly with increasing flow rate. Thus Table 5.1 shows an increasing heat flux with increasing flow rate. Another similar observation is that as the vapor fraction in the fracture increases the heat flux decreases, while the temperature of the saturated fluid in the fracture remains the same.

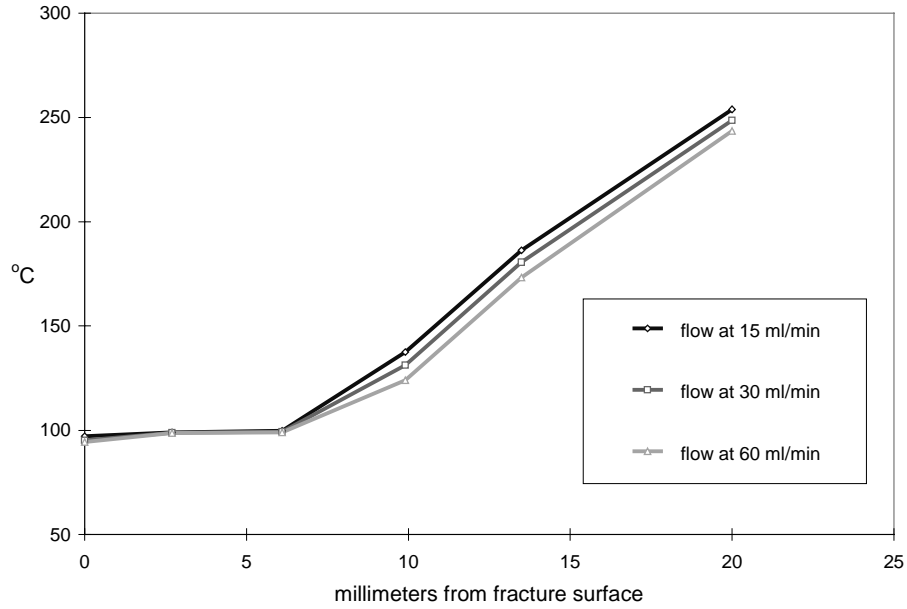


Figure 2.5. Steady state temperature gradients with boiling flow in sandstone disk.

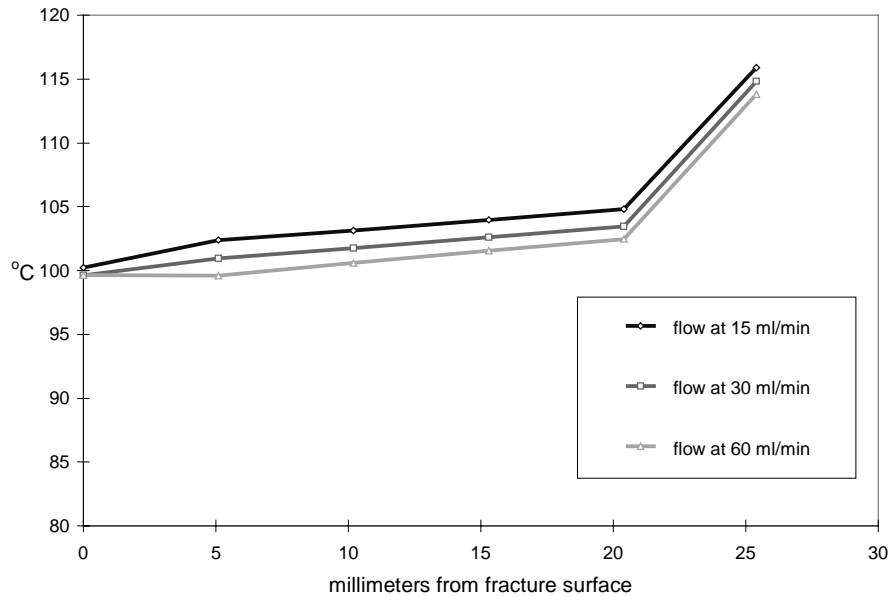


Figure 2.6. Steady state temperature gradients with boiling flow on aluminum disk.

Table 5.1 lists the heat fluxes calculated from an assumed thermal conductivity of each material. The vapor fractions listed were observed visually, not measured. It is interesting to note that the low porosity, low permeability graywacke showed little variation in heat flux as a function of flow conditions. As noted earlier, the aluminum and sandstone, chosen for their extremes of no porosity and high porosity, have different heat flux trends. As the vapor fraction increases and flow rate decreases, the heat flux to

the aluminum surface decreases. However, with sandstone, as the vapor fraction increases and the flow rate decreases, the heat flux increased, apparently because the surface was boiling more uniformly at lower flow rates.

Flow rate, ml/min	Vapor fraction, %	Heat flux, W/m <sup>2</sup>
Geysers core		
15 ml/min	40 %	24500 W/m <sup>2</sup>
30 ml/min	20 %	
60 ml/min	10 %	25100 W/m <sup>2</sup>
Aluminum disk		
15 ml/min	85 %	27400 W/m <sup>2</sup>
30 ml/min	60 %	28500 W/m <sup>2</sup>
60 ml/min	30 %	32300 W/m <sup>2</sup>
Sandstone		
15 ml/min	95 %	34800 W/m <sup>2</sup>
30 ml/min	85 %	31400 W/m <sup>2</sup>
60 ml/min	35 %	22900 W/m <sup>2</sup>

*Table 5.1. Heat fluxes calculated from assumed thermal conductivity and internal temperature gradients.*

## **2.5 DISCUSSION**

Because the heat flux sensors failed, the magnitude of the heat fluxes is somewhat uncertain, however, the relative magnitudes have been compared correctly. In these experiments porous and nonporous materials behave quite differently. The nonporous aluminum shows sensitivity to the flowing conditions in the fracture. The high porosity sandstone is sensitive to flow conditions in the rock itself, but not to the flow conditions in the fracture. The low porosity and low permeability Geysers graywacke also behaves unlike the other two materials. The temperature gradient indicates that vaporization occurs slightly beneath the fracture surface, isolating the boiling in the pores from the flow conditions in the fracture. But low permeability in this rock also prevents the flow in the fracture from extending very far into the matrix.

The thermal conductivity calculated from the temperatures and heat flux in the ice water experiment is notably lower than most measurements of conductivity in Geysers rocks (Walters and Combs, 1991). Thermal conductivity is a moderate function of temperature, but in porous materials where the pores can be occupied either by liquid or vapor the thermal conductivity may change significantly as the rock is heated. During the boiling experiments the temperature at the base of the rock exceeded the saturation temperature

and the conditions there may have been vapor-dominated. This would lead to overestimates of the heat fluxes.

For the graywacke and sandstone, an extrapolation of the linear trend from the middle of the rock disk to the saturation temperature of 100°C indicates the depth within the rock that liquid is circulating, vaporizing, and returning to the fracture. This idea is illustrated by the boiling temperature gradient of the Geysers graywacke shown in Figure 2.7. In this figure the arrow indicates the location where boiling within the rock alters the temperature gradient to the fracture surface.

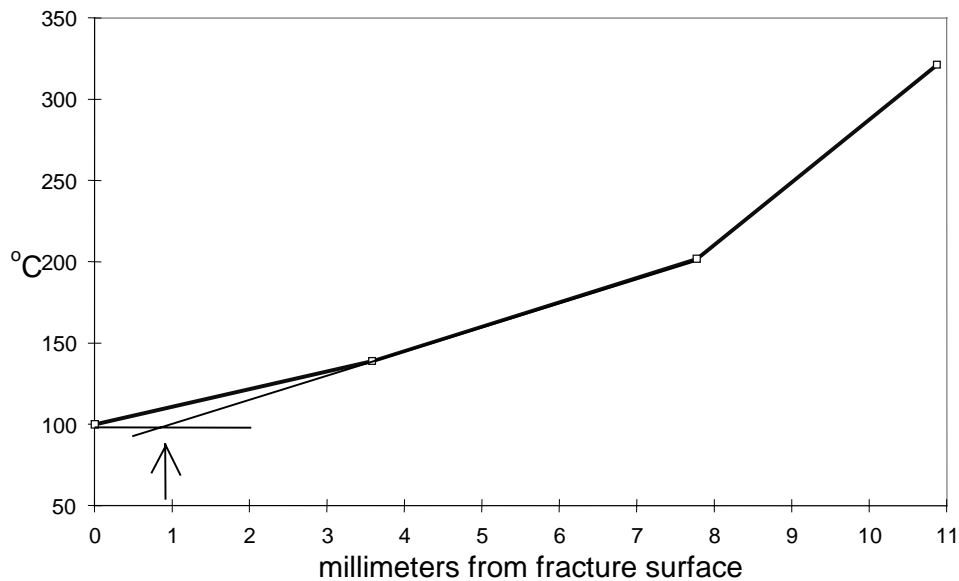


Figure 2.7. Extrapolated temperature gradient assuming uniform thermal conductivity.

One conclusion that can be drawn from this illustration is that boiling in a fracture is not strictly a surface phenomenon even in very low porosity and low permeability rock, but that the rock porosity and permeability play important roles in either reducing or enhancing the coupling between the heat flux and the liquid/vapor ratio of the flow in the fracture.

## **2.6 CONCLUSIONS**

A comparison of data indicates that while heat transfer on nonporous surfaces is strongly coupled to the flow regime and vapor fraction, the heat flux from porous rock surfaces with boiling appears to be much less sensitive to the quantity of vapor flowing in the fracture. The thermodynamics of vaporization in porous media follow the excess temperature  $\Delta T_e$  required for boiling, and the heat flux is influenced by matrix permeability as well as porosity. These experiments need to be reproduced more carefully conducted with working heat flux sensors, and the liquid-vapor fractions exiting the fracture should be measured more precisely.

## **2.7 FUTURE RESEARCH**

The direction of future work will begin with reproducing the recent experiment, focussing on eliminating the uncontrolled and unmeasured elements. These include solving the heat flux sensor operation problem, quantifying the liquid-vapor fractions exiting the fracture, and eliminating the flow discontinuities at the radial edge of the fracture. We will also repeat the experiment with Geysers core rock, prepared in a fashion similar to the more recently used aluminum and sandstone. One disk, with multiple holes for thermocouples, will be used rather than the previous method using several stacked disks.

### **3. EXPERIMENTAL DETERMINATION OF ENDPOINT SATURATION**

This project is being conducted by Research Assistant, Rodolfo Belen Jr. and Prof. Roland Horne. The aim is to determine experimentally the endpoint saturation of the steam-water relative permeability curves in Geysers reservoir rocks.

#### **3.1 BACKGROUND**

Relative permeability is important in describing the flow of two-phase steam and water in geothermal reservoirs. Presently, however, relative permeability relations for steam and liquid water are not fully understood. Permeability relations are normally adopted from field data or from nitrogen and water flow experiments.

The experimental determination of steam and liquid water relative permeabilities is a central target of the Stanford Geothermal Program. Experiments on Berea sandstones were performed by Ambusso (1996) and Satik (1998) made use of X-ray computer tomography to measure steam saturations. In a different approach, numerical simulation was used by Guerrero, Satik and Horne (1998) to infer relative permeabilities of Berea sandstones, based on temperature, pressure, heat flux and steam saturation data from dynamic boiling experiments performed by Satik (1997). X-ray CT scanning was also used to measure the saturation distributions within the core samples in these experiments. Flow-through experiments are currently being performed by Mahiya (see Section 1) to determine steam and liquid water relative permeability relations of Berea sandstones. Thin film heating elements that are transparent to X-rays will be used as guard heaters in these experiments to monitor and control heat losses from the core. As a consequence, adiabatic conditions will be maintained during the experiments.

All of these earlier studies used Berea sandstone in order to capitalize on the larger permeability, which enabled the experiments to be performed in reasonable time. This study aims to extend the understanding to low permeability geothermal rocks by determining just the endpoint saturations of the relative permeability curves. The endpoint or irreducible saturation of a certain phase is the saturation at which that phase becomes mobile in multiphase flow. Combining information about the endpoint saturations from the (slow) geothermal rock experiments with information of the general shape of the relative permeability curves from the (faster) sandstone rock experiments will completely define the steam-water relative permeability behavior. Determination of the irreducible water saturation of Geysers rocks would provide a better understanding of the adsorption characteristics of these rocks and will be valuable in accurately estimating reserves of the Geysers field.

Several experiments have been performed in the past to study the adsorption characteristics of Geysers rocks. BET (Brunauer, Emmett and Teller) type apparatus was used initially for the high-temperature adsorption measurements (White, 1973; Hsieh, 1980; Hsieh and Ramey, 1983; Herkelrath, 1983; and Luetkehans, 1988). However, these experiments took a very long time to reach equilibrium because the core samples



that were used had poor porosity and permeability. This long equilibrium time resulted in valve leakages and were believed to have introduced significant errors in the experimental results (Herkelrath, 1983).

Experiments were then performed using an automated, high temperature sorptometer that made use of crushed rock samples. Adsorption and desorption isotherms of Berea sandstone and Geysers core were studied by Shang, Horne and Ramey (1994). Initial and final pressures were measured at each adsorption/desorption step and were used to calculate the adsorbed/desorbed water at each step by material balance. The experiments used crushed core samples to reduce experiment run time and leakages at elevated temperatures. Experimental results were inconclusive and additional experiments using Geysers core samples were recommended. Experimentation was then continued by Satik, Walters and Horne (1995) using 36 Geysers core samples. The goal was to construct an adsorption map of the Geysers field. However, experimental results indicate that rock properties such as porosity, surface area and pore size distribution are only weakly correlated with the adsorption properties of the rock samples.

The amount of adsorbed water in these experiments were then converted to water saturation values using Equation 3.1.

$$S_w = \frac{1 - \phi}{\phi} \frac{\rho_r}{\rho_w} q \quad (3.1)$$

where  $\phi$  is the porosity,  $q$  is the amount of adsorbed water,  $\rho_r$  and  $\rho_w$  are the densities of the rock and water respectively. An approximate range of values for the irreducible water saturation of the core samples can be deduced from the water saturation values corresponding to the point when bulk condensation begins, i.e., when system pressures approach the saturation pressures of water at the system temperature. The calculated water saturations varied greatly with the rock properties and the range was between 0.2 and 0.4.

### **3.2 FUTURE PLANS**

After reviewing previous studies on relative permeabilities and water adsorption of Berea sandstone and Geysers cores, it is intended to modify the procedure of the dynamic boiling experiment of Satik (1997) and use these for the experimental determination of end-point saturation of Geysers rocks. As the first step, the results of the dynamic boiling experiment will be analyzed to check if endpoint saturations can be deduced from the experimental data obtained. The experimental apparatus and procedures will then be modified accordingly.

The following is a brief description of the boiling experiment of Satik (1997). The experimental apparatus consisted of an epoxy core holder containing Berea sandstone, a data acquisition system and a balance to measure inflow and outflow. The core was

initially evacuated and then saturated with deaerated water. The core was insulated with a fiber blanket to minimize heat losses in the radial direction. The heater was attached to the bottom of the core and was insulated with ceramic fiberboard. The heating end of the core was closed to fluid flow while the other end was connected to a water reservoir placed on a balance that was used to monitor the amount of water leaving the core during the experiment. Pressure, temperature and heat flux were measured in the core using pressure transducers, thermocouples and heat flux sensors respectively. Steam saturation was measured at every 1-cm increment along the core using the X-ray CT scanner. Heat input rate was increased every time steady state conditions were reached which means that no more water was coming out of the core and that the pressure, temperature and heat flux values had stabilized.

#### **4. REFERENCES**

Ambusso W.J., 1996. Experimental Determination of Steam-Water Relative Permeability Relations, MS Thesis, Stanford University, Stanford. Calif.

Ambusso W., Satik C., Horne R. (1996), "A Study of Relative Permeability for Steam-Water Flow in Porous Media", Proceedings of 21<sup>st</sup> Workshop on Geothermal Reservoir Engineering, Stanford University, Stanford, California.

Guerrero M., Satik C., Finsterle S., and Horne R. (1998), "Inferring Relative Permeability From Dynamic Boiling Experiments", Proceedings of 23<sup>rd</sup> Workshop on Geothermal Reservoir Engineering, Stanford University, Stanford, California.

Mahiya G. and Horne R. (1998), "Measurements of Steam-Water Relative Permeability", Stanford Geothermal Program Quarterly Report April-June 1998, Stanford University, Stanford, California.

National Instruments Corporation, 1994, SCXI-1163R User Manual, Product documentation, Austin, TX

National Instruments Corporation, 1996, Introduction to SCXI, Product documentation, Austin, TX

Satik C., and Horne R. (1995), "An Experimental Study of Adsorption in Vapor Dominated Systems", Proceedings of 20<sup>th</sup> Workshop on Geothermal Reservoir Engineering, Stanford University, Stanford, California.

Satik C. (1996), "Adsorption Characteristics of Rocks from the Vapor-Dominated Geothermal Reservoir at the Geysers CA", Proceedings of 21<sup>st</sup> Workshop on Geothermal Reservoir Engineering, Stanford University, Stanford, California.

Satik C. (1997), "Experiments of Boiling in Porous Media", Proceedings of 22<sup>nd</sup> Workshop on Geothermal Reservoir Engineering, Stanford University, Stanford, California.

Satik C. (1998), "A Measurement of Steam-Water Relative Permeability", Proceedings of 23<sup>rd</sup> Workshop on Geothermal Reservoir Engineering, Stanford University, Stanford, California.

Shang S., Horne R., Ramey H. Jr. (1995), "Water Adsorption on Geothermal Reservoir Rocks", Geothermics 24(4), 523-540.